14th International Symposium on Turbulence and Shear Flow Phenomena (TSFP14)
Heidelberg, Germany, July 28–31, 2026

LAGRANGIAN RELATIVE MOTION OF PARTICLE-BUBBLE PAIRS IN THREE-PHASE FLOWS

Tian Ma, Hendrik Hessenkemper, Guangyuan Huang
Institute of Fluid Dynamics
Helmholtz-Zentrum Dresden – Rossendorf
Dresden, 01328, Germany
email: tian.ma@hzdr.de

Andrew D. Bragg
Department of Civil and Environmental Engineering
Duke University
Durham, NC 27708, USA

ABSTRACT

We report the first experimental study of bubble–particle pair dispersion in an initially quiescent liquid. To this end, we simultaneously track deformable bubbles, finite-sized inertial particles (glass beads), and tracers in 3D by combining our in-house Lagrangian bubble tracking tool with the dense particle tracking algorithm OpenLPT. The experiment is performed in an octagonal bubble column, where a homogeneously distributed bubble swarm rises in water, generating a flow field representative of a three-phase bubble column (e.g., flotation cells). Tracer data reveal that the addition of glass beads enhances turbulence at large scales, while leaving the small-scale (sub-bubble) fluctuations essentially unchanged. From the trajectories of bubbles and inertial particles, we compute the mean squared separation (MSS) of bubble–particle pairs. The results show that dispersion follows the classical ballistic regime at short times (MSS $\propto t^2$), transitioning to a diffusive regime at longer times (MSS $\propto t$). Notably, at long times, bubble–particle pairs disperse faster than both particle–particle and bubble–bubble pairs. This enhanced dispersion is explained using the dispersion angle—the angle between the relative velocity and separation vectors—highlighting more efficient alignment in bubble–particle pairs than in the other cases.

Introduction

Bubble–particle relative motion plays a central role in mixing, transport, and collision processes in many natural and industrial gas–liquid–solid flows. For example, in flotation cells, the relative velocity between bubbles and particles determines the approach of fine mineral particles to the bubble surface, directly influencing recovery rates. Most existing knowledge of three-phase flow physics is based on Eulerian measurements, which provide statistics at fixed points in space. In recent years, however, Lagrangian techniques capable of following the trajectories of individual bubbles and particles have become feasible even in relatively dense bubbly flows (Ma *et al.*, 2025). A key quantity in the Lagrangian description of bubble–particle interactions is the relative pair dispersion, defined by the separation $r(t) = \|\mathbf{x}_b(t) - \mathbf{x}_p(t)\|$, where $\mathbf{x}_b(t)$ and $\mathbf{x}_p(t)$ denote the positions of a bubble and a particle at time t. Understanding the dynamics of $r(t)$ is essential for describing bubble–particle encounters and collisions, which underpin fundamental processes of transport and mixing in three-phase turbulence. This study addresses this issue by providing the first experiment of bubble–particle (here, bubble-bead) relative dispersion in a controlled three-phase flow.

Experimental method

The three-phase experiments were conducted in an octagonal bubble column (Fig. 1) with a diameter of 11.5 cm and a water height of 90 cm. Bubbles were injected through eight needle spargers at the bottom. By varying the needle size and gas flow rate, we generated different cases of monodisperse, homogeneous bubbly flows. The bubbles were relatively large ($3 \sim 5$ mm), producing substantial turbulence and increasing the scale separation between d_b and η, thereby favoring the emergence of a K41 regime (Ma *et al.*, 2025). The gas void fraction α was adjusted to maintain all cases within the homogeneous bubbly flow regime while ensuring sufficient interactions between bubble wakes.

Measurements were performed in a region of 4.5 cm $\times$ 4.5 cm $\times$ 9 cm, recorded with four calibrated high-speed cameras at 2500 frames per second over 30 s. The measurement volume was located at $z = 50$ cm above the injection plane, ensuring that bubbles entering the field of view had lost memory of their injection conditions. By combining our in-house 3D Lagrangian bubble tracking tools (Hessenkemper *et al.*, 2024) with the dense particle tracking algorithm OpenLPT (Tan *et al.*, 2020), we simultaneously tracked bubbles, glass beads, and tracers in 3D. The glass beads had a diameter of 0.4 mm, density $\rho_p = 2.5 \times 10^3$ kg/m^3, and void fraction $\alpha_p \approx 0.1\%$. The tracers were 100 μm polyamide particles. To our knowledge, this is the first experimental realization of fully 3D simultaneous Lagrangian tracking of three phases, including dense deformable bubbles.

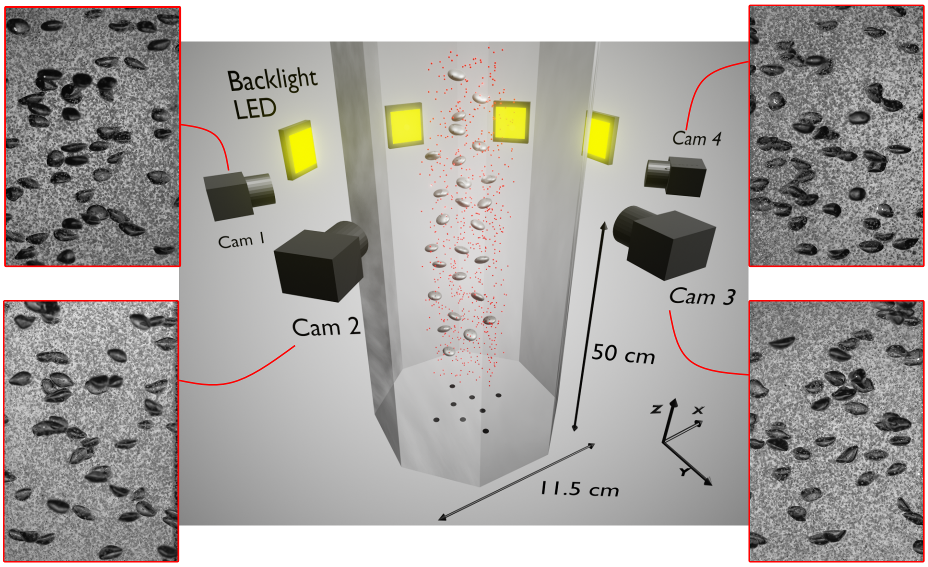

Figure 1. Sketch of the octagonal bubble column used in the experiments (note that in the actual experiment, the number of bubbles in the column is $O(10^3)$ and approximately 50 to 100 bubbles are tracked in the field of view). The red points in the center panel present glass beads.

Preliminary results

We present preliminary results for the case with bubble size $d_b \approx 4.4$ mm and void fraction $\alpha_b = 1.2\%$. For comparison, we conducted a reference case with only settling beads and no bubbles. In addition, a two-phase bubble-only reference case is taken from our previous experiments with identical d_b and α_b, i.e. the *La* case reported in Ma *et al.* (2025) and Huang *et al.* (2025).

Figure 2 shows the second-order longitudinal structure function of tracers in the three-phase case, the bubble–liquid two-phase case (labeled as 2-Phase (Bubbles)), and the bead–liquid two-phase case (labeled as 2-Phase (Beads)). (Note: D_{LL} of the 2-Phase (Beads) case are not yet fully converged; work is ongoing to improve this dataset). We find that turbulence in the column is predominantly generated by bubbles. In the present three-phase setup, the addition of glass beads enhances turbulence at large scales, whereas for $r < d_b$, D_{LL} remains nearly unchanged compared to the bubble-induced turbulence (BIT) in the two-phase reference case.

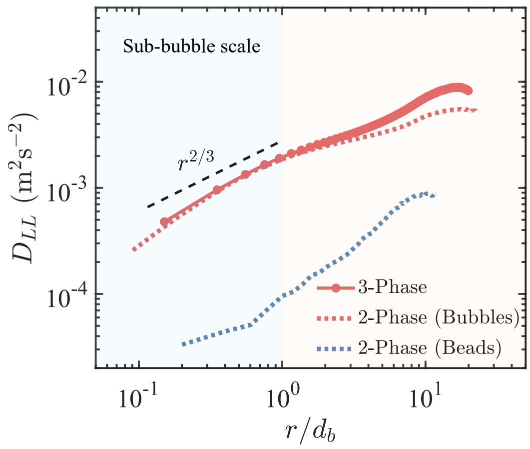

Figure 2. Second-order longitudinal structure function $D_{LL}(r)$ of tracers for three cases: three-phase (bubbles + glass beads), two-phase bubble–liquid ("2-Phase (Bubbles)"), and two-phase bead–liquid ("2-Phase (Beads)"). Note: D_{LL} of the 2-Phase (Beads) case are not yet fully converged.

Figure 3 shows the mean-squared separation $\langle \|r - r_0\|^2 \rangle$ of bubble-bead pairs as a function of t, for initial separations $r_0 \equiv \|\mathbf{r}_0\| = 10d_b$. The data closely follows Batchelor's ballistic regime, $\langle \|r - r_0\|^2 \rangle \propto t^2$, which is supposed to be valid over the time for which the bubble-bead pair relative velocity remains approximately the same as that at the initial time $t = t_0$. At longer times, the dispersion magnitude follows the order: bubble–bead pairs $>$ bead pairs $>$ bubble pairs. This order can be explained using the dispersion angle θ (Shnapp *et al.*, 2023), defined as the angle between the relative velocity vector and the relative separation vector. For bubble pairs, θ oscillates around 90°, an inefficient configuration for separation. In contrast, θ for bead pairs and bubble–bead pairs converges toward 60°–70° and 30°–40°, respectively, corresponding to increasingly efficient alignments between relative velocity and separation.

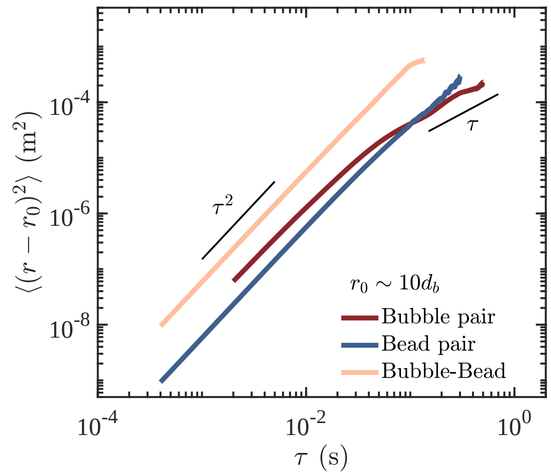

Figure 3. Mean-squared separation $\langle\|r-r_0\|^2\rangle$ of bubble-bead pairs as a function of t for initial separations $r_0 = 10d_b$, shown together with bead–bead and bubble–bubble pairs dispersion for comparison.

Conclusion and outlook

Using simultaneous 3D Lagrangian tracking of bubbles, inertial particles, and tracers, we examined the relative dynamics in a three-phase bubbly flow. We find that turbulence is predominantly generated by bubbles, while added beads enhance large-scale fluctuations without affecting sub-bubble scales. Pair-dispersion analysis shows a clear hierarchy: bubble–bead pairs disperse fastest, followed by bead pairs and bubble pairs. This ordering is linked to the dispersion angle, which controls the efficiency of velocity–separation alignment. These findings shed new light on the fundamental mechanisms of mixing and dispersion in multiphase turbulence and open the way for a deeper Lagrangian characterization of three-phase flows.

REFERENCES

Hessenkemper, H., Wang, L., Lucas, D., Tan, S., Ni, R. & Ma, T. 2024 3d detection and tracking of deformable bubbles in swarms with the aid of deep learning models. *Int. J. Multiphase Flow* **179**, 104932.

Huang, G., Hessenkemper, H., Tan, S., Ni, R., Sommer, A., Bragg, A. D. & Ma, T. 2025 Taylor dispersion of bubble swarms rising in quiescent liquid. *J. Fluid Mech.* **1014**, R1.

Ma, T., Tan, S., Ni, R., Hessenkemper, H. & Bragg, A. D. 2025 Kolmogorov scaling in bubble-induced turbulence. *Phys. Rev. Lett.* **134** (24), 244001.

Shnapp, R., Brizzolara, S., Neamtu-Halic, M. M., Gambino, A. & Holzner, M. 2023 Universal alignment in turbulent pair dispersion. *Nat. Commun.* **14** (1), 4195.

Tan, S., Salibindla, A., Masuk, A. U. M. & Ni, R. 2020 Introducing openlpt: new method of removing ghost particles and high-concentration particle shadow tracking. *Exp. Fluids* **61**, 1–16.